Journal of Coastal Research	SI 36	96-108	(ICS 2002 Proceedings)	Northern Ireland	ISSN 0749-0208

Spatial Variability of Wave Conditions on the French Atlantic Coast using In-Situ Data

Rémi Butel, Hélène Dupuis and Philippe Bonneton

D.G.O., UMR C.N.R.S. 5805 EPOC, Université Bordeaux I
Avenue des Facultés
33405 Talence Cedex
France

ABSTRACT

This study aims to provide a statistical description of wave conditions on the French Atlantic coast. The large scale spatial variability of sea states at the French Atlantic coast is assessed using wave rider time series at Biscarosse (in 26m depth) and l'ile d'Yeu (in 33m depth), about 300 km apart. The major differences between the two locations obtained from 3D histograms of significant wave heights, periods and directions indicate that (i) higher wave heights are encountered at l'Ile d'Yeu and (ii) larger range of wave directions and age at Biscarosse, mainly due to atmospheric forcing. The temporal variability at the two wave rider locations is shown by seasonal statistics, with two main seasons: October to March and April to September. Three types of data classifications are compared ; 12 classes allow the main encountered situations to be described.

ADDITIONALINDEX WORDS: *Swell, wind wave, data analysis, statistics, data classification.*

INTRODUCTION

Coastal dynamics is a developing research field due to the major role of coastal evolution on human activities and vice-versa: coastal areas are usually important for human activities such as economy and tourism, in return human beings create artificial structures that affect the fragile coastal equilibrium.

The physics involved in coastal research are usually more complicated than in open ocean due to the occurrence of non linear processes in intermediate to shallow water and resulting coupling with sediment transport (BAILARD, 1981).

Coastal evolution of beaches is affected by a variety of factors such as tidal currents, wave-induced currents which have different effects according to the bathymetry, topography and sediment properties. Hence, nearshore morphodynamics can be classified (WRIGHT and SHORT, 1983). Sandy coast are subject to very rapid and/or long-term evolution. Efforts have been made to understand and predict coastal dynamics, either at large time and space scales (HANSON, 1989), at intermediate scales (de VRIEND *et al*., 1993, ROELVINK and STIVE, 1989) or at smaller scales to better characterize processes (BONNETON, 2001 ; BONNETON and DUPUIS, 2001). In each case, the knowledge of hydrodynamics responsible for the coastal change is very important and data have to describe both the morphology of the coastal area and the corresponding forcing factors.

This study deals with an analysis of wave characteristics in the bay of Biscay, France, in connection with field experiments undertaken at Truc Vert beach supported by "Programme National d'Environnement Côtier". Different approaches of the coastal evolution have been undertaken to characterize the beach and its evolution: at small time scales, topographic surveys based on theodolite or a Differential Global Positioning System (DGPS) have been regularly carried out on a reference site of a few kilometres along the coast (WEBER 1978, MICHEL and HOWA, 1999, PEDREROS *et al.*, 1996). DGPS-surveyed coastlines enable mapping of the ridge and runnel systems. At larger scales, optical imagery of SPOT satellites have been used to characterize the coastlines on lengths of several tens of kilometers and in particular sub-tidal crescentic bars and ridge and runnel systems (LAFON *et al*., 2001).

Concerning hydrodynamics, all scales are also taken in to account using wave riders for large scales, Synthetic Aperture Radar images for meso-scale (DUPUIS *et al*., 1998) and pressure arrays for small scales in the surf zone (SENECHAL *et al*., 2001).

This study focuses on the larger scale wave variability which is necessary to identify the waves climate in the area. It aims to illustrate large spatial scale changes in the wave properties along the coast (the long term climatic temporal evolution is not evaluated). Also, it investigates extreme events probability which have drastic effects on the coastlines. Seasonal variability is elucidated from the results.

This study is based on in-situ measurements by wave riders using three devices (only one directional, in the other cases the direction of VAG-Atla model (GUILLAUME, 1987) is used to allow for directional information). They are located at Biscarosse (in 26m depth) and l'ile d'Yeu (in 33m depth), about 300 km apart along the coast, and Gascogne (in 4500m depth). Time series of wave parameters such as significant wave height and mean wave period include 2 to 20 years according to the location. This allows to update earlier studies in the area such as those of VASSAL (1980) which is very extensive but based on model outputs which may introduce bias, or those of WEBER (1978) which is based on short time series only.

To allow for determining wave characteristics that affect the coast, shallow water wave characteristics at about 5m should be considered. A wave propagation model should be run for the whole deep water dataset onto the continental shelf. Grouping of data, making use of classification of wave heights, periods and directions, has been devised as a method for the future as it proved very time consuming to conduct the analysis based on all wave combinations. Simulations of wave propagation from the sensor location to the shallow water depth will be only undertaken for the centers of gravity of the classification. Results obtained from 3 different classifications are discussed for each buoy location.

The paper is organised as follow: first we describe the different data sources, then the methods we apply. Results are then given, consisting in several kind of histograms, and the classification of sea states is presented, before discussion and conclusion.

MATERIALS

Figure 1 shows the geographical location of all data sources. This map shows that open ocean conditions exists in the following ranges:

- 260° to 335° for Biscarosse
- 225° to 315° for Yeu
- 200° to 360° for Biscay

There are also long fetch ranges for Yeu and Biscay:

- 170° to 225° for Yeu
- 0° to 200° for Biscay

Biscarosse

The Biscarosse buoy (a Datawell wave rider deployed by Centre d'Essai des Landes) is moored at 44.46° North, 1.32° West, on the continental shelf in 26m depth. Data, obtained by zero-crossing methods, have been available since year 1980 with discontinuous records. The first records, until year 1989, contain data for heights $H_{1/3}$, the sampling frequency is 3 hours. From 1990 to 2000, data contain the mean periods T_{mean} and additional paramenters not used here, and the sampling is generally done every 1/2 hour, but

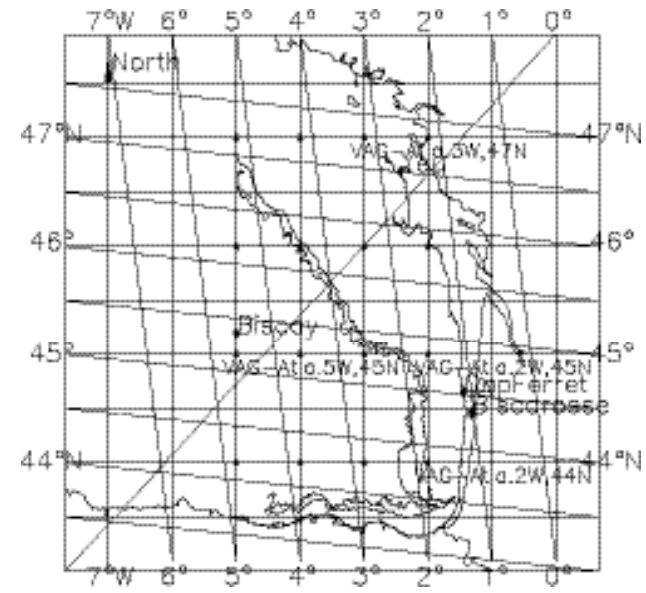

Figure 1 localization of data sources. The grid of output of the VAG-Atla model are shown by small diamonds. The position of wave riders are shown with greater diamonds. 4 isobathes are drawn: -50m, -200m, -400m, -1000m.

can range from 5 minutes to 1/2 hour. Data is not directional and availability is in general low for the winter months. An extensive review of the original data shows that there are very few data for years 1999 and 2000.

Yeu

The Yeu buoy (owned by Centre d'Etudes Techniques Maritime Et Fluvial : CETMEF) is moored at 46.691° North, 2.4275° West, on the continental shelf in 33m depth. Data are available from 1998/07/24 until 2000/01/15. These consist of the spectral parameters for significant wave heights, H_{m0}, the spectral mean periods, T_{02} and mean direction. Data are generally sampled every 3 hours and every hour in case of storm.

Biscay

Although the Biscay buoy is situated in deep water and far from the Atlantic French coast, it was considered interesting to study it in the same way than Yeu and Biscarosse, as sea states at Biscay can be useful as confirmation or forerunner for case studies and for seas state at the coast. The Biscay buoy is moored at 45.2° North, 5° West, in 4500m depth, deployed by French Meteorological Office (Météo-France) and United Kindom Meteorological Office (UKMO). In this study, data span the period from 1998/02/03 until 2001/12/12, for H_{sig} (the significant height), T_{mean}. Data is sampled every hour.

Table 1 avaibility of data for the different analyses and locations.

source	statistics	Number of samples	dates
Biscarosse	classification	3434	1996/01/01 -> 2000/09/11
Biscarosse	other statistics without direction	131098	1980/01/01 -> 2000/09/11
Yeu	all statistics	6325	1998/07/24 -> 2000/01/15
Biscay	classification	1373	1999/02/03 -> 2001/03/30
Biscay	other statistics without direction	12780	1999/02/03 -> 2001/03/30

VAG-Atla

The output of the Météo-France second generation wave model VAG-Atla (GUILLAUME, 1987), is located on a one by one degree grid. For each point the output consisted of Hsig, Tmean, and Dirmean, the mean direction on a given record of data, and a spectral decomposition in 3 components, a main swell, possibly a crossing swell, and wind waves. For the two points nearest of the Biscarosse buoy in our data base these data are available from April 1996 to October 2000, for the full Gulf of Biscay they are available from May 1999 to October 2000.

As the wave direction does not exist for Biscarosse and Biscay buoys, we chose to pick out the VAG-Atla output at one of the the nearest point from the Biscarosse buoy. The correlation coefficient between wave directions for the points 2°W, 44°N and 2°W, 45°N is 0.963. Given the strong relationship, the direction at Biscarosse point can be well estimated by the output of VAG-Atla at point 2°W, 45°N. For the Biscay buoy, point 5°W, 45°N was used.

METHODS

Preprocessing

The data sets included some spurious data due to erroneous measurements. To correct this a procedure was devised using the following criteria for data elimination:

- wave height greater than 15 meters,
- wave period greater than 25 seconds,
- wave period lower than 1 second,
- combined wave period lower than 3 seconds and height greater than 1 m,
- wave height increase greater than 2 meters per hour,
- wave period increase greater than 3 seconds per hour.

These thresholds were established after a close examination of raw data. As a result for the Biscarosse buoy, for example, 86.7 % of the 151247 initial values were selected (131098).

Completing

Data were stored in a data base and, using a related tool box (BUTEL, 2000), accessed for different kinds of analysis, then displayed. This tool box provides, in particular, a way to unify two sets of measurement dates, in order to compare dates from different sources. For classification, at each item of the data set 3 pieces of information are used, i.e. 3 coordinates, the significant height, the mean period and the mean direction of waves.

Weighting

As data are not evenly distributed in time (due to absence of measurements, bad data or unequal measurement duration), they have to be weighted. Following TUCKER (1991), all statistics presented in this paper are weighted (i) by a monthly factor, $\mathrm{Max}(D_{month}) / D_{month}$, where Dmonth is the cumulated duration of measurements for a given month, (ii) by a sample to sample weighting factor, Di, duration accounted for a piece of data.

To take in account the fact that D_i may vary, each measurement weighted by a factor which is simply $D_i * \mathrm{Max}(D_{month}) / D_{month}$. Resulting data after weighting is summarized in Table 1.

Histograms

Statistics for the 3 localizations were carried out, including: 1-D histograms for height and period; cumulative probability distribution that enable to estimate extreme conditions; 1-5D histograms for directions with heights; statistics computation; and bivariate histograms. Weibull-3 fitting (TUCKER 1991) is given for cumulative distribution. The Weibull-3 formula is:

$$P(x) = 1 - \exp\left(-\left(\frac{x-\hat{c}}{\hat{a}}\right)^{\hat{a}}\right) \quad (1)$$

Bivariate Histograms

Bivariate histograms, plotting the probability density in function of Tmean and Hsig, provide complementary information: ages of waves (and steepness) allow to classify them in developing, well developed wind seas and swell. When range of periods narrows for the higher values of height, they can give an estimate of the mean parameters of extreme sea-state. On these bivariate histograms two different plots are added: First plotting the centers of gravity of the classes obtained by classification; this point will be discussed later. Second, curves of particular relation between Tmean and H_{sig} are plotted:

- fully developed seas using the PIERSON-MOSKOWITZ formulas (1964) giving - in deep water - a constant steepness, g=Hsig/L of 1/19.7 (where L is wave length) :

$$H_{sig} = 0.021 \; U_{10}^{\;2} \tag{2}$$

$$T_{mean} = 0.518 U_{10} \tag{3}$$

- developing wind seas, using JONSWAP formulas integrated by CARTER (1982), with D being the duration of the wind blow, and U10 the wind speed at 10m height (m/s):

$$H_{sig} = 0.0146 * \; D^{0.6} * U_{10}^{\;0.8} \tag{4}$$

$$T_{mean} = 0.540 * \; D^{0.37} * U_{10}^{\;0.47} \tag{5}$$

In this case the curve showing the dependence of Hsig as a function of Tmean is computed by solving the equations (4-8), for any given wave age, with h the water depth:

$$C_p = Age * U_{10} \tag{6}$$

$$C_p = L/T \tag{7}$$

$$C_p = \frac{gL}{2\partial} \tanh\left(\frac{2\partial h}{L}\right) \tag{8}$$

Classifications

We use three different methods in order to classify sea states, and to obtain a given number of sea states at each buoy. First the distance between states must be established. Coefficients of covariance are computed over the set of data. Then the generalized distance is given as specified in DAGNELIE (1975).

$$\vec{A}\left(\begin{vmatrix} H_{sig1} \\ T_{mean1} \\ Dir_1 \end{vmatrix}, \begin{vmatrix} H_{sig2} \\ T_{mean2} \\ Dir_2 \end{vmatrix}\right) = \sqrt{\frac{(H_{sig1}-H_{sig2})^2}{S_{Hsig}^{\;2}} + \frac{(T_{mean1}-T_{mean2})^2}{S_{Tmean}^{\;2}} + \frac{(Dir_1-Dir_2)^2}{S_{dir}^{\;2}}} \tag{9}$$

where subscripts 1 and 2 correspond to two sea state samples, and sj^2 is the variance for j parameter.

There is a natural function (hereafter denoted total in this paper) to measure the quality of a classification, following BELAÏD and BELAÏD (1992):

$$total(P) = \sum_{Cg \in P} \sum_{x \in C} dist(x, Cg) \tag{10}$$

where P is any given partition, C any class in this partition, Cg the center of gravity of class C, and x any point of this class. Thus, the classification becomes an optimization problem on the coordinates of gravity centers of classes.

As quoted in MODULAD (1987), classification methods are split in two parts: choice of the initial distribution of classes, then iterations to adjust the repartition of the points in the classes.

The computations carried out demonstrate the variability of results depending on the initialization step. Hence the function total is used to measure the quality of each classification, keeping in mind that a global optimum is hard to find, and that all methods give only local optimum.

Ball and Hall method

Given an a-priori distance d_0, points of the data-set are classified using the following rule: if the distance between the point and the center of gravity of all existing classes is greater than d_0, then a new class containing this point is formed, else it is added to the nearest class and the new gravity center of this class is computed. Adjusting the a-priori distance d_0 allows to obtain partitions with almost any given number of class.

Forgy method

This method has been devised by FORGY (1965). Given a subjective set of points, it uses at first step as center of gravity of subjective classes (thus giving a fixed number of resulting classes), the following process is iterated until convergence is achieved: for each class, empty the set of constituting points; for each point, find the nearest class gravity center, and add this point to the set of points of the class. When all points are classified, compute new gravity center of every class. The process stops when every displacement of gravity center are lower than a given epsilon.

If no data aggregate to a subjective initial point, this class is replaced by the center of gravity of the whole set, modified by a small incremented displacement. This particular algorithm is a variant of the LBG algorithm (LINDE *et al*., 1980).

Applying Forgy method 3 different initializations were used. The first taking for values the result of the Ball and Hall classification, the second taking for values the global center of gravity plus an incremented epsilon (LBG algorithm), and the third an arbitrary set of points obtained from a visual classification.

Classification method by simulated annealing minimization

The algorithm used here was described in GOFFE *et al*. (1994). Simulated annealing is an optimization method that allows to escape from local optima, in order to find a global optimum. The process is iterative, and consists of evaluations of the function total to minimise followed by a choice: when there is a decrease in the function value, the step is always accepted and the process goes on from this new point, and when there is an increase, the step is accepted under condition, thus enabling to escape from local optima. The decision to step uphill is made using a criterium, which makes step smaller and smaller. If the function value is stated as an energy, uphill and downhill of this energy are similar to the energy variation in an annealing.

RESULTS

1-D histograms for height and period

Heights

Figure 2 shows the weighted significant wave height probability distribution for the three data sets, corresponding statistics are in displayed in Table 2. Although maximum significant height is higher at Biscarosse than at Yeu (due to longer period of analysis), mean encountered H_{sig} is greater for Yeu (1.81m) than for Biscarosse (1.36m). The narrower distribution is the one of Yeu. The standard deviation is found 25% higher at Biscarosse. Biscay has much more higher values (2.64m) and a wider range with maximum wave heights of 14m.

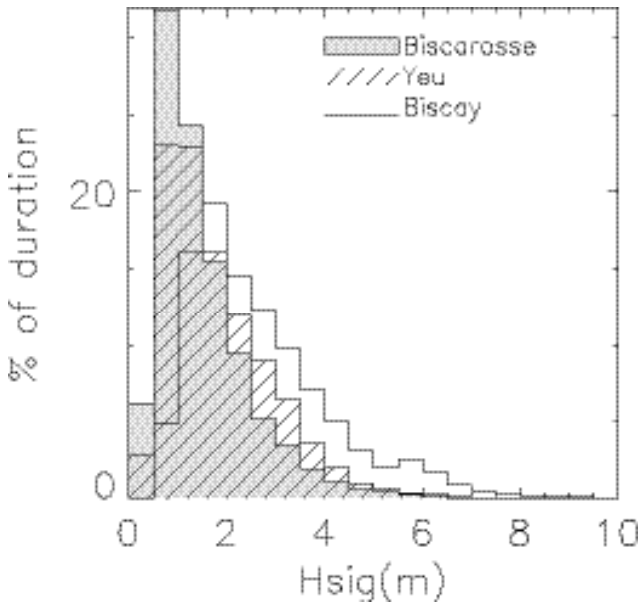

Figure 2 1-D histograms of Hsig. Gray shade is for Biscarosse, dashed surface is for Yeu, and white with thick lines is for Biscay.

Figure 2 Annual and seasonnal statistics for Hsig(m) with minimum, maximum, mean, median, standard deviation, skewness and simple distribution.

source	season	min.	max.	mean	med.	st.dev.	skew.	0..2M	2..4M	>4M
Biscarosse	annual	0.1	9.7	1.36	1.1	0.87	1.57	82.23%	16.47%	1.29%
	winter	0.1	6.4	1.57	1.4	0.94	1.25	75.50%	22.28%	2.21%
	spring	0.1	9.3	1.18	1	0.76	1.97	88.39%	10.83%	0.78%
	summer	0.1	8.1	1.09	0.9	0.65	2.32	92.42%	7.17%	0.41%
	autumn	0.1	9.7	1.6	1.4	0.97	1.1	72.33%	25.87%	1.81%
Yeu	annual	0.22	8.88	1.81	1.52	1.07	1.19	65.22%	30.62%	4.16%
	winter	0.45	6.3	2.15	2.04	0.99	0.77	48.57%	46.95%	4.47%
	spring	0.25	6.39	1.55	1.36	0.9	1.15	73.44%	24.67%	1.89%
	summer	0.22	5.48	1.35	1.1	0.83	1.59	83.52%	15.08%	1.40%
	autumn	0.46	8.88	2.16	1.9	1.2	1.09	53.90%	38.27%	7.83%
Biscay	annual	0.2	13.9	2.64	2.3	1.45	1.27	43.38%	41.42%	15.20%
	winter	0.8	9.5	3.09	2.7	1.52	1.15	28.76%	50.35%	20.89%
	spring	0.2	6.4	2.04	1.9	1	1.12	57.40%	37.87%	4.73%
	summer	0.5	7.7	1.82	1.6	0.95	2.02	74.09%	22.12%	3.79%
	autumn	0.4	13.9	3.43	3.2	1.46	1.03	15.63%	56.01%	28.36%

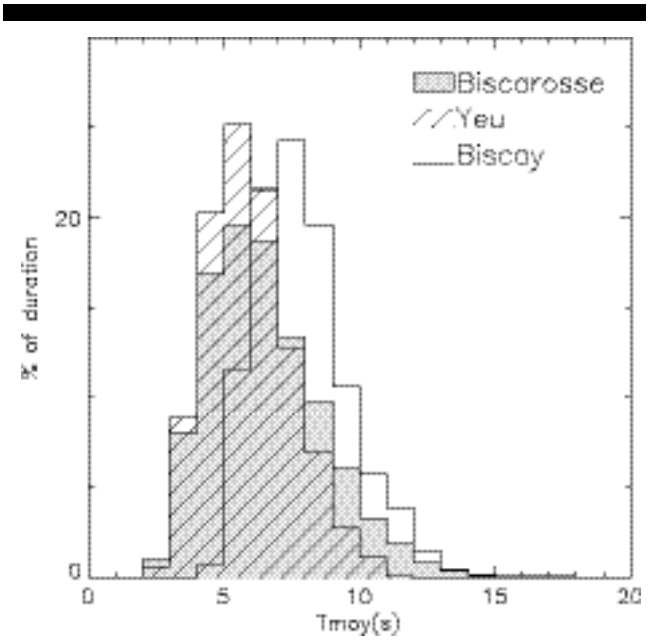

Figure 3 1-D histograms of Tmean. Gray shade is for Biscarosse, dashed surface is for Yeu, and white with thick lines is for Biscay.

Periods

Figure 3 and table 3 show the Tmean weighted distribution for the three data sets. Mean annual periods are smaller for Yeu (5.9s) than for Biscarosse(6.5s). The shift is of 0.6s. So it seems that waves at Yeu are younger waves (wind waves), than at Biscarosse (assessed by further analysis, with bivariate histograms). The narrower distribution is the one of Yeu. Biscay mean annual period is 7.37s.

1-5D histograms for direction

Figures 4a,b,c show the directional histograms for each of the 3 sources. The gray scale allows to display the Hsig wave classification in three classes with thresholds of 1.5m and 3m.

Figure 4a is obtained for Biscarosse height coupled with VAG-Atla direction. It shows 3 principal sectors, from W-WNW to NW-NNW. Figure 4b is obtained from Yeu data. The two main sectors are WSW-W and W-WNW (52%). Figure 4c is obtained for Biscay height coupled with VAG-Atla direction at point 5W,45N. It shows 4 principal sectors, from WSW-W to NW-NNW.

While the direction of higher waves at Yeu is obtained for the WSW-W sector, at Biscay and Biscarosse they are respectively obtained for the WNW-NW and W-WNW sectors. 3 factors can induce this fact:

- variation of topography (wave propagation in intermediate water depth),
- as pointed out in Figure 1, open ocean condition have a larger direction range for Biscay and Biscarosse than for Yeu,
- trajectories of low pressure centers are generally situated at North of Biscay buoy.

Table 3 Annual and seasonnal statistics for Tmean(s) as in Table 2. The periods given by the Biscay buoy are in seconds, with no decimal part.

source	season	min.	max.	mean	med.	st.dev.	skew.	0..9S	9..13S	>13S
Biscarosse	annual	1.7	25	6.5	6.2	2.17	1.11	87.86%	11.39%	0.75%
	winter	1.7	25	7.5	7.4	2.61	0.64	73.74%	23.87%	2.40%
	spring	1.9	25	5.8	5.5	1.83	2.08	95.54%	4.22%	0.24%
	summer	2	22	5.81	5.6	1.61	0.98	95.66%	4.26%	0.07%
	autumn	2.2	22.5	6.94	6.8	2.01	0.47	85.71%	13.94%	0.36%
Yeu	annual	2.4	12.1	5.89	5.7	1.55	0.49	96.11%	3.89%	0%
	winter	2.8	12.1	6.81	6.67	1.66	0.23	88.46%	11.54%	0%
	spring	2.8	10.5	5.54	5.4	1.37	0.54	98.55%	1.45%	0%
	summer	2.4	10.5	5.18	5.1	1.18	0.6	99.42%	0.58%	0%
	autumn	2.9	11.1	6.18	6.25	1.5	0.09	96.68%	3.32%	0%
Biscay	annual	1	25	7.37	7	1.73	0.79	88.39%	11.50%	0.11%
	winter	1	25	8.00	8	1.80	0.76	81.09%	18.67%	0.24%
	spring	2	13	6.65	7	1.34	0.68	97.33%	2.67%	0%
	summer	4	13	6.51	6	1.32	0.88	97.65%	2.35%	0%
	autumn	4	18	8.1	8	1.66	0.58	80.68%	19.18%	0.14%

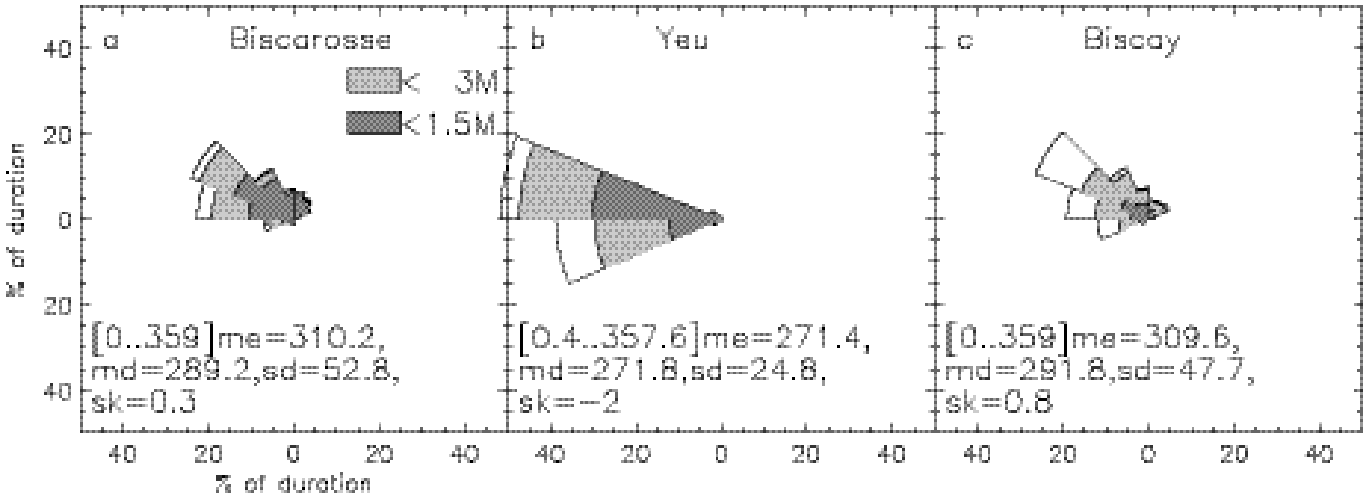

Figure 4 Histograms 1.5-D of the mean wave direction. Each sector is 22.5° wide. The percentage accounts for the duration in each sector. Gray scale is the following: dark gray for direction when height is lower than 1.5m, light gray when height is lower than 3m, and white for height over 3m. « me » stands for mean, « md » for median and « st » for standard deviation.

Extreme conditions

Cumulative probability distribution of the three data sources are plotted in Figure 5, including Weibull-3 fitting. It can be noted that the adjustments of Biscarosse and Yeu join for big height. Cumulated probability curve transformed to return period are displayed (for 1, 5, and 10 years). As return dashed lines apply to duration of events of 1 hour, heights of 7m (resp. 8 and 12m) are then statistically observed every year at Biscarosse (resp. Yeu and Biscay).

The fit for DPS-5 model distribution studied by VASSAL (1980) is also plotted, with the dashed-dotted line, with a modification to take in account that our plotted data are $H_{1/3}$, while the DPS-5 data used are $H_{1/10}$. The point studied by VASSAL corresponds to the Biscarosse buoy location. With the DPS-5 model, VASSAL (1980) obtained similar extreme conditions than we find with the Yeu buoy up to significant wave heights of 5m. The increase of his second adjustment can be partly due to the fact dans DPS-5 is a deep water model. The decrease of wave height from Biscay buoy to the coast is very clear. Indeed there is no more than 1hour of Hsig equal to 10m every 10 years at Biscarosse while these heights are obtained several times a year at Biscay.

The bivariate histograms help to provide the wave steepness in these extreme conditions.

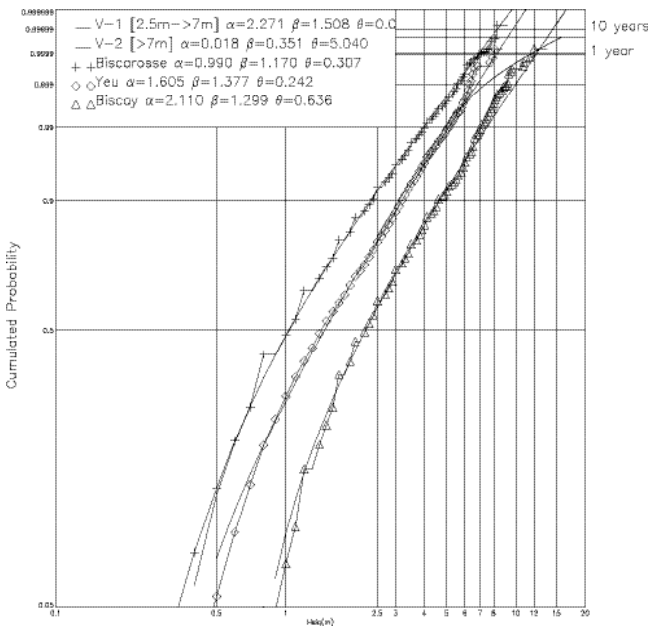

Figure 5 Cumulative probability distributions. Scales are in X-Log, in Y-Log-Log(1/(1-P(x)). Weibull-3 fitting are superimposed in each case, displayed by solid lines. Plus, diamonds and triangles correspond respectively to Biscarosse, Yeu and Biscay data. The Weibull-3 fittings by VASSAL(1980) is displayed by the dash-dotted lines. These cumulated probability enable to estimate the return period. Three dashed lines respectively for 1 year, 5 years and 10 years are displayed on the right vertical axis.

Bivariate histograms

Biscarosse

The bivariate histogram (Figure 6) shows that at Biscarosse seas states are mainly swell conditions, with high wave age or low steepness (indeed there is a very low probability for H_{sig} to be on the right hand of the curve of wind wave in equilibrium, from the PIERSON-MOSKOVITZ formula). Moreover, the steepness of 1/48 characterize the annual mean of T_{mean} and H_{sig} (51% of the data lie below this curve). Also, because both the wave height and period are positively skewed (See Tables 2 and 3), the maximum of probability is located in the lower part of the graph, while contour levels are elongated on the right and top parts.

Yeu

Figure 7 shows the bivariate T_{mean} x H_{sig} histogram at Yeu. As the curve for the wave age of 1.2 almost fits the maxima in the frequency distribution, Yeu has the largest number of case of wind waves. For H_{sig} greater than 2m, there are as many case of developing seas as swell cases. The steepness of the mean annual parameter is 1/30 (52.6% of the data lie below this curve).

Biscay

Figure 8 shows the bivariate T_{mean} x H_{sig} histogram. Here distribution of wave age is intermediate: for the whole range of H_{sig} there are both developing sea conditions and swell states.

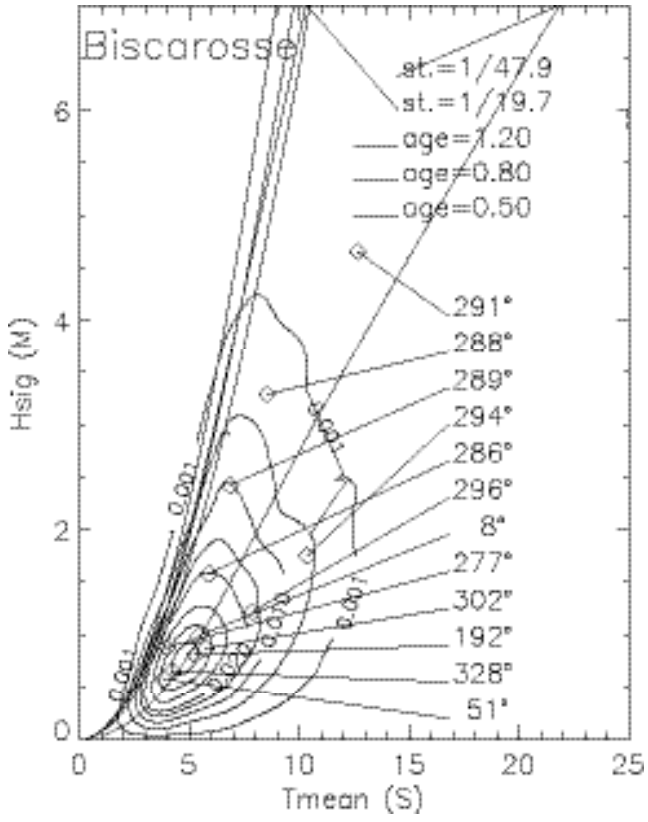

Figure 6 Bivariate histogram of Tmean versus Hsig at Biscarosse. Contour lines are plotted for values of 0.001, 0.005, 0.01, 0.015, 0.02, 0.03, 0.04, 0.05, 0.1, 0.2, 0.3, and 0.4 % of duration, first dashed, then thicker and thicker. Solid lines are drawn for wind sea age of 0.8, 1.0, and 1.2. Dashed lines are drawn for constant steepness, the first one for center of the histogram, the second one for the PIERSON-MOSKOVITZ curve. White diamonds are the locations of the center of gravity given by the classification. They are linked to their mean direction.

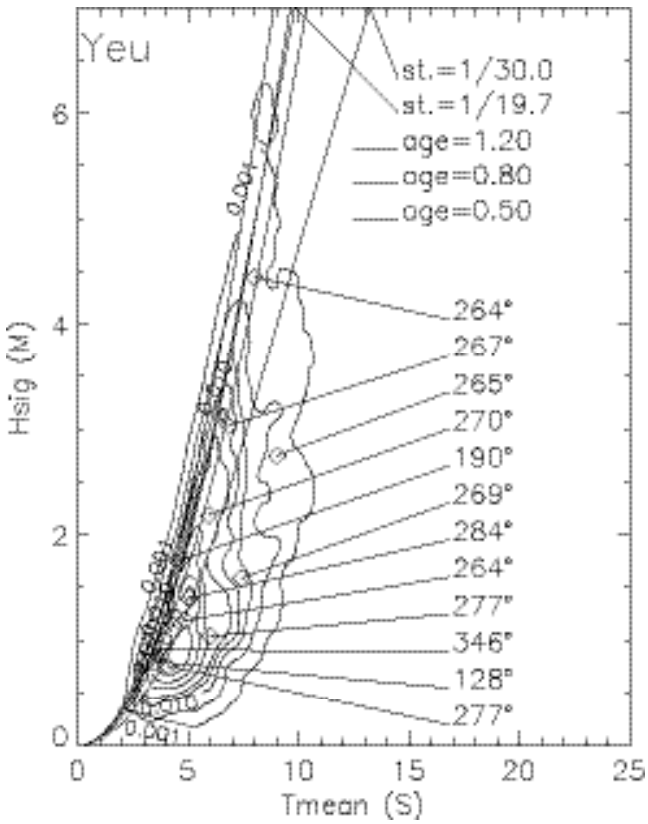

Figure 7 Bivariate histogram of Tmean versus Hsig at l'Ile d'Yeu. See Figure 6 explanations.

Seasonal distribution

Previous section describes the global statistics of sea states. However, at latitudes of 44°N to 47°N, large inter-annual variability could be expected.

Table 2 and 3 show the statistics for the heights and periods, for each quarter in a year, which was found to be sufficient, based on monthly analysis. Two main seasons are observed, hereafter called winter (October to March) and summer (April to September).

At Biscarosse, the winter mean height is about 1.6m (75 % lower than 2m) while the summer one is about 1.1m (90% lower than 2m). The mean periods decreases by 1.4s between summer and winter.

At Yeu the winter mean height is about 2.2m (50% lower than 2m), while the summer one is about 1.45m (78% lower than 2m). The mean period decreases by 1.1s.

At Biscay the winter mean height is about 3.25m (22 % lower than 2m), while the summer one is about 1.9m (65 % lower than 2m). The mean period decreases by 1.5s.

It should, however, be noted that extreme events can appear at any time.

Summary of spatial variability

At Biscarosse, heights are the lowest, and wave ages are the largest. So the wave steepness are the lowest, mainly associated with swell. At Yeu, there are more wind waves (wave period is smaller), especially for high waves, than at Biscay where there are a little more swell states. Also at Yeu, the main direction is West (52 % of situation are in a 22.5° narrow sector WNW), while at Biscarosse the main direction is NW. This is due to the fact that the Yeu location is nearer to the air pressure gradients and high wind speeds associated with low pressure. At this location wind and wave directions are more aligned, while at Biscarosse the swell arrives due to the wave directional spreading at the storm location (generally with a delay of the order of 10 to 20 hours compared to Yeu). For a 300km distance between Yeu and Biscarosse, periods have a 0.6s (10%) shift down while Hsig are 33% higher at Yeu.

CLASSIFICATION

Comparison of methods

The 3 dimensional sea state vectors make impossible classification without using systematic (objective) methods. The choice of a given method is itself almost subjective. So we had to compare methods using an objective criterium, the total function.

In Table 4 scores are given for the different classifications and initialization methods. In all cases the simulated annealing gives a better score than other methods. The simulated annealing method takes about 1300 seconds to perform 111601 iterations on a 866MHz Pentium III PC, so the efficiency of this method is proven. It is also more robust to changes of initialization.

12 classes were used, as a compromise between a too redundant classification and a classification that do not contains class for extreme conditions.

Table 4 Classification scores.

location	method	total	nb-iters.
Biscarosse	Ball and Hall	1776.86	1
Biscarosse	Forgy/init=arbitrary	1334.39	32
Biscarosse	Forgy/init=c.g.	1339.78	66
Biscarosse	Forgy/init=H and B	1340.32	85
Biscarosse	sim.ann.	1307.52	111601
Biscay	Ball and Hall	541.86	1
Biscay	Forgy/init=arbitrary	434.60	27
Biscay	Forgy/init=c.g.	436.19	22
Biscay	Forgy/init=H and B	450.83	28
Biscay	sim.ann.	423.33	111601
Yeu	Ball and Hall	1160.00	1
Yeu	Forgy/init=arbitrary	1072.93	66
Yeu	Forgy/init=c.g.	1078.60	63
Yeu	Forgy/init=H and B	1070.82	75
Yeu	sim.ann.	1058.89	108001

Table 5 Simulated annealing classification for Biscarosse. O.O. means open ocean conditions, L.F. means long fetch conditions and S.F. means short fetch conditions. "e.w.w" stands for equilibrium wind wave sea. The class 4 waves does not affect the coast.

id.	number	of points	Hsig	Tmean	Dir	Type Sea state
1	482	0.87	5.76	302.01	O.O.	summer swell, WNW, 0.9m, 5.8s
2	420	1.22	7.87	296.41	O.O.	annual swell, W, 1.2m, 7.9s
3	382	0.65	4.24	328.43	O.O.	summer swell, NW, 0.7m, 4.2s
4	343	0.58	3.84	51.58	S.F.	annual swell, W, 02.6m, 3.8s
5	342	1.58	5.90	286.58	O.O.	annual swell, W, 1.6m, 5.9s
6	328	2.42	6.85	289.56	O.O.	annual swell, WNW, 2.4m, 5.4s
7	313	0.99	5.42	8.87	L.F.	annual swell, N, 1m, 10s
8	253	0.88	3.96	277.24	O.O.	summer e.w.w., W, 0.9m, 4s
9	191	1.75	10.36	294.76	O.O.	winter swell, WNW, 1.8m, 10.4s
10	180	3.29	8.55	288.26	O.O.	winter big swell, S, 3.3m, 8.6s
11	176	0.81	5.25	192	L.F.	annual swell, WNW, 0.8m, 5.3s
12	47	4.66	12.66	291.8	O.O.	winter big swell , WNW, 4.7m, 12.5s

Table 6 Classification for l'Ile d'Yeu. "d.w.w" stands for developing wind waves.

id.	number	of points	Hsig	Tmean	Dir	Type Sea state
1	1491	3.03	6.84	267.58	O.O.	winter e.w.w. W 3m 6.8s
2	948	2.19	5.94	270.25	O.O.	annual e.w.w. W 2.2m 6s
3	714	4.45	8.00	264.58	O.O.	winter e.w.w. W 4.5m 8s
4	579	0.76	4.06	277.91	O.O.	summer swell W 0.8m 4.1s
5	513	1.04	5.99	277.02	O.O.	summer swell W 1m 6s
6	485	1.19	4.86	264.45	O.O.	annual swell W 1.2m 4.9s
7	470	1.40	5.03	284.19	O.O.	summer swell WNW1.4m 5s
8	463	2.75	9.04	265.85	O.O.	winter swell W 2.8m 9s
9	447	1.59	7.43	269.73	O.O.	annual swell S 1.8m 4.7s
10	83	1.76	4.67	190.07	L.F.	annual d.w.w. S 1.8m 4.7s
11	68	0.80	3.46	128.51	L.F.	annual e.w.w. SE 0.8m 3.5s
12	64	0.91	3.43	346.29	O.O.	annual d.w.w. NNW 0.9m 3.4s

Table 7 Simulated annealing classification for Biscay.

id.	number	of points	Hsig	Tmean	Dir	Type Sea state
1	197	1.32	5.75	310.96	O.O.	summer swell NW 1.3m 5.8s
2	149	1.61	5.77	265.62	O.O.	summer swell W 1.6m 5.8s
3	140	2.75	6.97	278.46	O.O.	annual swell W 2.8m 7s
4	134	1.47	7.12	292.24	O.O.	summer swell WNW 1.5m 7.1s
5	123	1.21	5.39	357.10	O.O.	summer swell N 1.2m 5.4s
6	119	2.75	8.31	303.73	O.O.	winter swell NNW 2.8m 8.3s
7	117	1.86	7.16	336.91	O.O.	annual swell NNW 1.9m 7.2s
8	101	4.04	8.05	292.37	O.O.	winter e.w.w. WNW 4m 8.1s
9	96	2.26	6.17	48.83	L.F.	winter e.w.w. NE 2.3m 6.2s
10	80	1.29	5.00	55.18	L.F.	summer swell NE 1.3m 5s
11	63	5.64	10.20	299.70	O.O.	winter swell WNW 5.6m, 10.2s
12	54	3.01	10.62	308.98	O.O.	winter swell NW 3m 10.6s

Results from the simulated annealing method

The monthly distribution of each class (not shown here) was found helpful to characterize the classes and determine if a class is annual or seasonal, as indicated in last columns of Tables 5 to 7.

The classifications systematically identify the classes with the highest wave heights as winter classes, confirming the previous seasonal analysis.

Figures 6 to 8 display the distribution of the centers of gravity of classes obtained with the simulated annealing solver (diamond symbol). The labels plotted give the mean direction of the class. The number of points of each class can be found in associated Tables 5 to 7. It must be noted that these centers of gravity convey another piece of information: the mean direction. For example, in Figure 6, 3 neighbour centers over the 1/48 curve account for 3 very different directions: 192°, 302° and 8°.

Classification for the Biscarosse buoy

Table 5 displays the 12 classes obtained for Biscarosse. For half classes, sea states belongs either to winter (October to March) sea states, or summer ones. All classes but one have a steepness corresponding to swell (in most of the cases the location of the buoy is such that residual swells are always present in the spectra). The class with the highest H_{sig} has a very low steepness of 1/40, due to a period of 13s. Only 3 classes do not have open ocean condition (4, 7, 11). As their steepness is very low they probably correspond to mixed seas with superposition of wind wave and a swell component.

Yeu

Table 6 shows the 12 classes of Yeu sea states. Summer swell waves of sector West, (4.1s, 0.8m), (6s, 1m) and (5s, 1.4m) could be merged for morphodynamic studies. Directions are better grouped than at Biscarosse, in open ocean conditions. There are only two long fetch cases. The proportion of seasonal classes is the same as for Biscarosse. There are only three classes with directions not in the N-NW sector.

In the Yeu classification, half classes correspond to equilibrium or developping wind seas. Particularly, the class with the highest H_{sig} has much more higher steepness than Biscarosse one.

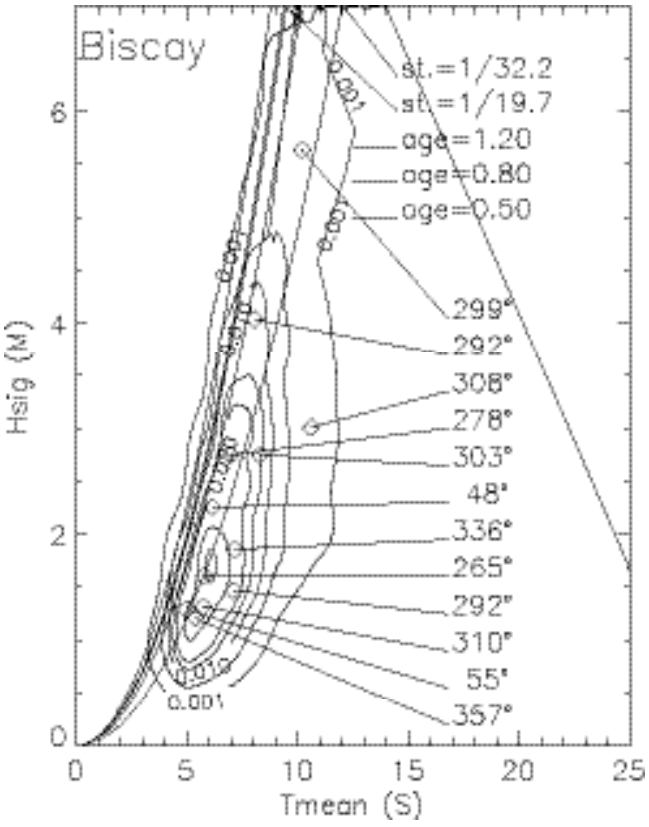

Figure 8 Bivariate histogram of Tmean versus Hsig at Biscay. See Figure 6 explanations.

Biscay

Table 7 shows the 12 classes for Biscay. The same kind of distribution in annual, winter and summer classification was found. There are two well developed wind sea classes and also two classes of East wind waves (wind waves and swell). The three classes of the higher H_{sig} corresponds to NW waves, coming from far.

The case of the highest waves corresponds partially to the 1999/12/27-28 storm.

DISCUSSION

Directions given by VAG-Atla

The lack of directional information at Biscarosse and Biscay buoys was made up by using directional information from the deep water depth VAG-Atla model. The validation of this model is in progress (it is already done for heights and periods). The correlation with a new buoy, a directional Triaxys, moored at Cap Ferret, will help in the validation process. Moreover, a correction is yet neglected: the refraction of the wave direction due to the effect of the slope of the continental shelf. As stated above, the classifications were developed with the aim of adjusting model and observations (using an intermediate water depth numerical model) and thus further validating VAG-Atla directions.

Heterogenous data base

Data availability take place at different times from years 1980 to 2001 (see Table 1). The bivariate histogram for Biscarosse is done without directional information from years 1990 to 2000, while on the same figure the plotted classes are done with directional information from years 1996 to 2000.

Drawbacks of the lack of data

A weak adjustment in fitting for extreme condition: lack points for severe conditions, but the results give a first approximation that is coherent with other studies.

A 3 months miss for Biscay classification : the zero gap seen for months February, March, April is due to the lack of VAG-Atla data in our data base, while the data for the Biscay buoy are available.

Classification issues

Even if the simulated annealing method gives the best scores, it cannot be assumed that the global minimum is found, that is only a better local minimum.

Since only global wave parameters are used while long distance swells are mainly observed, some classes may in fact gather different conditions including or not mixed seas. Also, aiming at providing the different wave conditions for sediment transport studies, the classifications may suffer from a lack of classes for the most energetic conditions. For example, one could add a class at (8.5s, 6m) for the Yeu location which would correspond to a developing energetic wind sea.

CONCLUSION

This study describes the statistical properties and the spatial variability of waves in the bay of Biscay (France). It provides a classification based on significant wave height, mean period and direction (with 12 classes) at three buoy locations, aiming to define the main sea states that affect the coast. The simulated annealing method gives the best results for classification. The statistical analysis shows that over a 300 km distance separating the northern buoy of Yeu and the southern buoy of Biscarosse, the wave conditions are modified. Indeed, the southern part is mainly concerned with very low steepness waves (mean annual Hsig and period of 1.4m and 6.5s), associated with long distance swells traveling mainly from N-NW directions (using the PIERSON and MOSKOWITZ (1964) criterion, only 1% (10%) of sea states correspond to pure wind waves respectively at Biscarosse (and Yeu)). We believe that Biscarosse buoy experiences mostly the same wave events (with a delay and energy and frequency decay related to the long distance travel) than the Yeu buoy (mean annual Hsig and Tmean of 1.8m and 5.9s). The differences in wave directions would partly be due to direction spreading from the low pressure centers. The Biscay buoy is moored in deep water and exhibites the highest wave heights (mean annual Hsig and period of 2.64m and 7.37s), partly due to its more exposed location. At the three locations, a strong seasonal cycle is observed with similar wave statistics over October to March and April to September.

This study indicates that more detailed analyses based on directional spectra would be useful at least for the Southern part of bay of Biscay where complex sea states with super-imposition of swell and wind seas are prevailing, in order to further characterize sea states and predict associated sediment transport and coastal evolution. This will be made possible using the new Triaxys direction wave rider (Axys technologies) installed the 28th of August 2001 a few tens of kilometers north of the Biscarosse buoy (together with a Datawell device for inter-comparison). It will be also useful to further validate the VAG-Atla model.

Further analysis of wave spatial variability but at smaller scale is undertaken based on Synthetic Aperture Radar images.

ACKNOWLEDGMENTS

This study was supported by Programme National d'Environnement Côtier. We are very gratful to the "Centre d'Etudes Techniques Maritime Et Fluvial" who developed the CANDHIS wave data base and provided the Yeu wave data. We also wish to thank the French Met. Office "Météo-France" for the VAG-Atla outputs extracted from the wind-flux AVISO data base, the "Centre de Météorologie Marine, Brest" and Service Hydrographique et Océanographique de la Marine for the Biscay wave data and, finally, the "Centre de Météorologie Marine, Biscarosse" and the "Centre d'Essai des Landes" for the Biscarosse wave buoy data.

LITERATURE CITED

BAILARD, J. A., 1981. An energetics total load sediment transport model for a plane sloping beach. *J. Geophys. Res*., 86, (C11), 10938-54.

BALL, G.H. and HALL, D.J., 1967. A clustering technique for summarizing multivariate data. *Behavior Science* 12, 153-155.

BELAÏD, A. and BELAÏD, Y., 1992. *Reconnaissance des formes Méthodes et applications*. InterEditions, 430p.

BONNETON, P. 2001. A note on wave propagation in the inner surf zone, *C. R. Acad. Sci. Paris*,vol 329, Série II b, pp. 27-33.

BONNETON, P., and DUPUIS, H., 2001. Transformation of irregular waves in the inner surf zone. *Proc. 27th Int. Conf. on Coastal Eng*, vol 1, pp. 745-754.

BUTEL, R. 2000. BOTIDO, une Boite à Outils pour le Traitement et l'Imagerie des Données de bouées Océanographiques, *Rapport interne* D.G.O., 35p.

CARTER D.J.T., 1982. Prediction of wave height and period for a constant wind velocity using the JONSWAP results. *Ocean Engineering* 9, pp. 17-33

DAGNELIE, P., 1975. *Analyse statistique à plusieurs variables*. Les Presses agronomiques de Gembloux, diffusion Vander-Oyez.362p.

DE VRIEND, H.J., ZYSERMAN, J., NICHOLSON,J., ROELVINK,J. A.,PÉCHON,P. and SOUTHGATE, H.N., 1993. 1993 Medium-term 2DH coastal area modeling. Coastal *Engineering*, 21, 193-224.

DUPUIS, H., FORGET, P., LAFON, V., and FROIDEFOND, J.M., 1998. Spatial distribution of swell wave properties in a coastal area using satellite images. *Oceans'98, IEEE conference*, Nice, 28 September - 1 October 1998, IEEE Cat. Nb. 98CH36259 / ISBN 0-7803-5047-2.

FORGY, E.W., 1965. Cluster analysis of multivariate data: efficiency versus interpretability of classifications, paper presented at biometric society meetings, Riverside, California, abstracts in *Biometrics*, vol 21, No 3, p. 768.

GOFFE, FERRIER AND ROGERS, 1994, Global optimization of statistical functions with simulated annealing, *Journal of Econometrics*, vol. 60, no. 1/2, Jan./Feb., pp. 65-100.

GUILLAUME, A., 1987. VAG, modèle de prévision de l'état de la mer en eau profonde, *Note de travail de l'EERM* No. 178, Direction de la Météorologie Nationale, 128p.

HANSON, H., 1989. GENESIS-a generalized shoreline change numerical model. *Journal of Coastal Research*. vol 5 (1), 1-27.

LAFON, V., DUPUIS, H., HOWA, H. and FROIDEFOND, J.M., 2001. Determining ridge and runnel long-shore morphodynamics using SPOT imagery, Submitted at *Oceanologica Acta*, Juillet 2001.

LINDE, Y., BUZO, A., and GRAY, R.M., 1980. An algorithm for vector quantized design. *IEEE Transactions on Computer* 28(1):p84-95.

MICHEL, D., HOWA, H., 1999. Short term morphodynamics response of a ridge and runnel system on a meso-tidal sandy beach. *Journal of Coastal Research*, 15, No 2, 428-437.

MODULAD, 1987. *ECOLE MODULAD*, méthodes de classification pour l'analyse des données. Institut National de Recherche en Informatique et en Automatique, 35p.

PEDREROS, R., HOWA, H. and MICHEL, D., 1996. Application of grain size trend analysis for the determination of sediment transport pathways in inter-tidal areas. *Marine Geology* 135, 35-49.

PIERSON, W.J. and MOSKOWITZ, L., 1964. A proposed spectral form for fully developed wind seas based on the similarity theory of S.A. Kitaigorodskii. *Journal of Geophysical Research*, 69, 5181-5203.

ROELVINK, J.A. and STIVE, M.J.F. 1989. Bar-generating cross-shore flow mechanisms on a beach. Journal of Geophysical Research, 94 (C4), 4785-4800.

SENECHAL, N., DUPUIS, H., BONNETON, P., HOWA, H., and PEDREROS, R., 2001. Irregular wave transformation in the surf zone over a gently slopping sandy beach, *Oceanologica Acta* (sent to press).

TUCKER, M.J. 1991. *Waves in ocean engineering: measurement, analysis, interpretation*. Chichester, England: Ellis Horwood Ltd, 430p.

VASSAL, J.P., 1980. *Les houles exceptionnelles et leurs conséquences*. Thesis, Université Bordeaux I, 199p.

WEBER, O., 1978. *Transits sédimentaires et évolution saisonnière de la zone littorale à la Salie (Gironde)*. Thesis, Université Bordeaux I, 126p.

WRIGHT, L.D., and SHORT A.D., 1983. Morphodynamics of beaches and surf zones in Australia. In *hand book of coastal Processes an Erosion*, P.D.Komaer Ed., pp.35-64 Boca Raton, FL: CRC Press.